Supplementary Information

Achieving Stable Syngas Production during Photothermal synergistic Dry Reforming of Methane over Layered Double Hydroxides-Based Catalysts with anti-coking Performance

Juntao Li[a], Tengfei Li[a], Yuhao Liu[a], Yang Guo[a,*], Lingzhao Kong[b,c], Pengjie Miao[b,*]

[a] *Key Laboratory of Thermo-Fluid Science and Engineering, Ministry of Education, School of Energy and Power Engineering, Xi'an Jiaotong University, Xi'an, Shaanxi 710049, PR China*

[b] *Xinjiang Key Laboratory of New Energy and Energy Storage Technology Xinjiang Institute of Technology, Aksu 843100, PR China*

[c] *School of Environmental Science and Technology, Suzhou University of Science and Technology, Suzhou, Jiangsu 215009. PR China*

Corresponding author: Y. Guo

E-mail: guoyang@xjtu.edu.cn ORCID ID: 0000-0001-9830-5942

Contents

Supplementary data

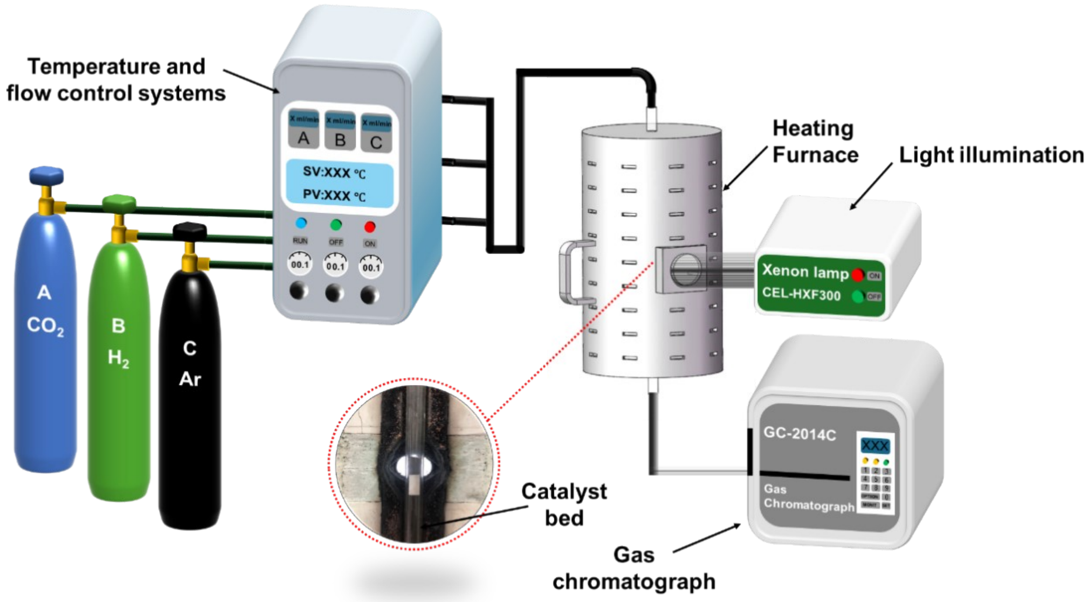

Figure S1. Overall Process Flow Diagram of the System.

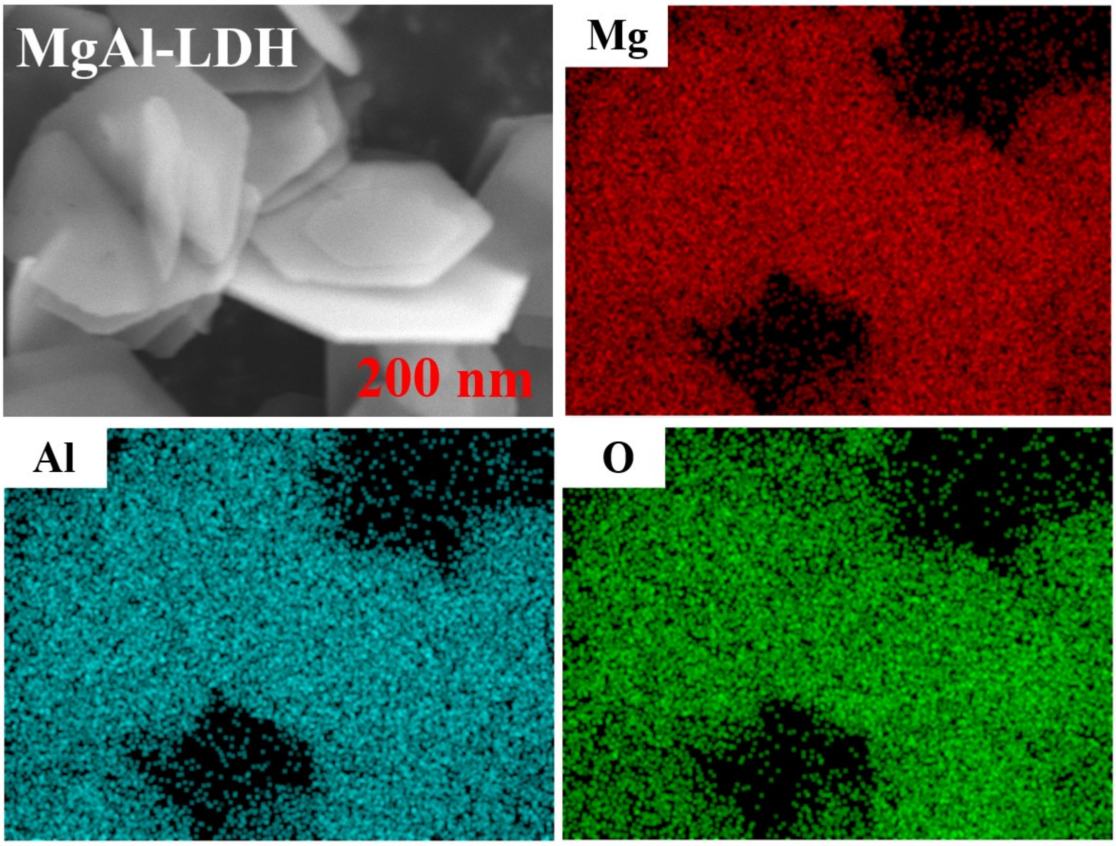

Figure S2. EDS image of MgAl-LDH.

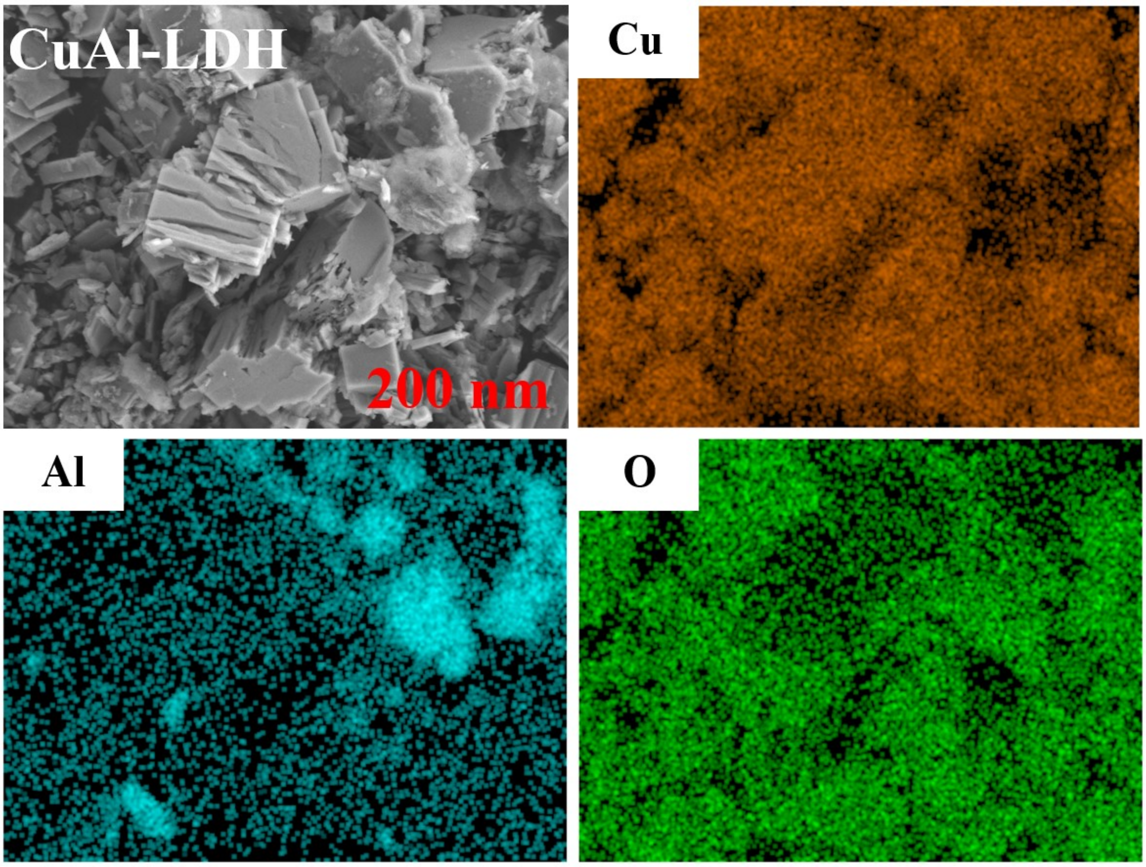

Figure S3. EDS image of CuAl-LDH.

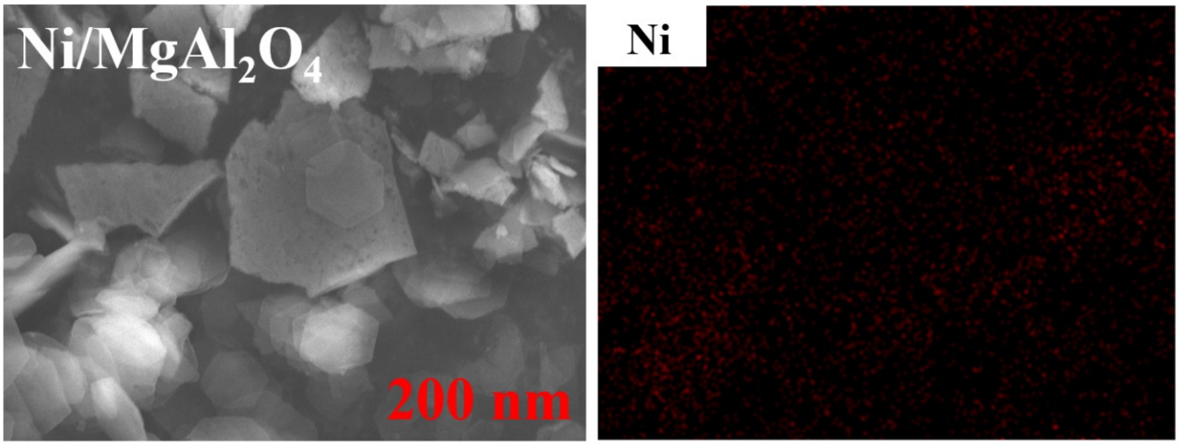

Figure S4. EDS image of $Ni/MgAl_2O_4$.

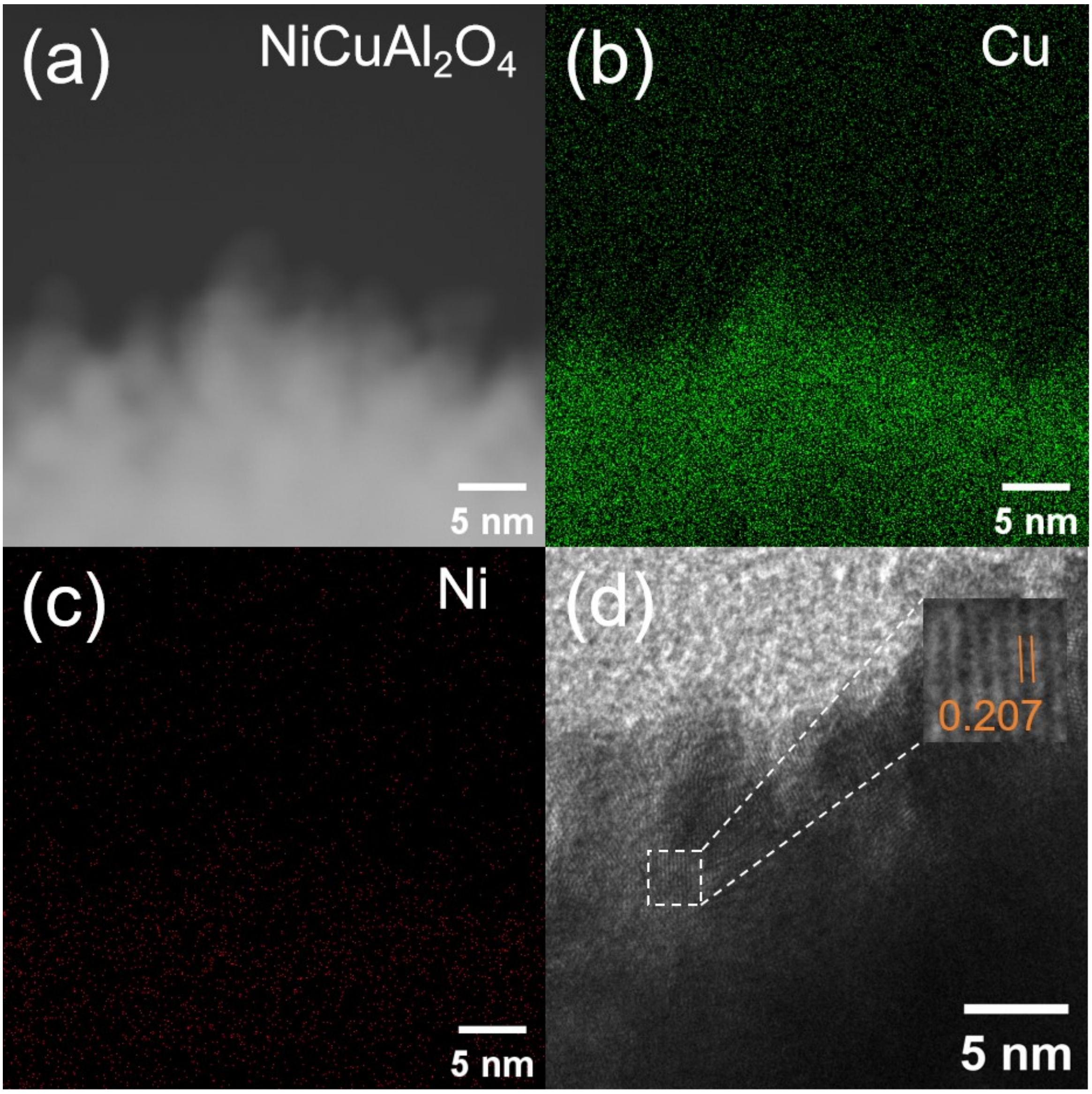

Figure S5. TEM characterization of the Ni/$CuAl_2O_4$ catalyst: (a) structural morphology; (b) EDS elemental mapping of Cu; (c) EDS elemental mapping of Ni; (d) lattice fringe spacing.

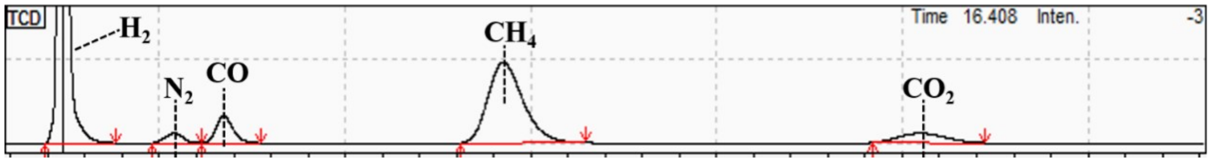

Figure S6. Gas chromatography sample diagram of the reaction product.

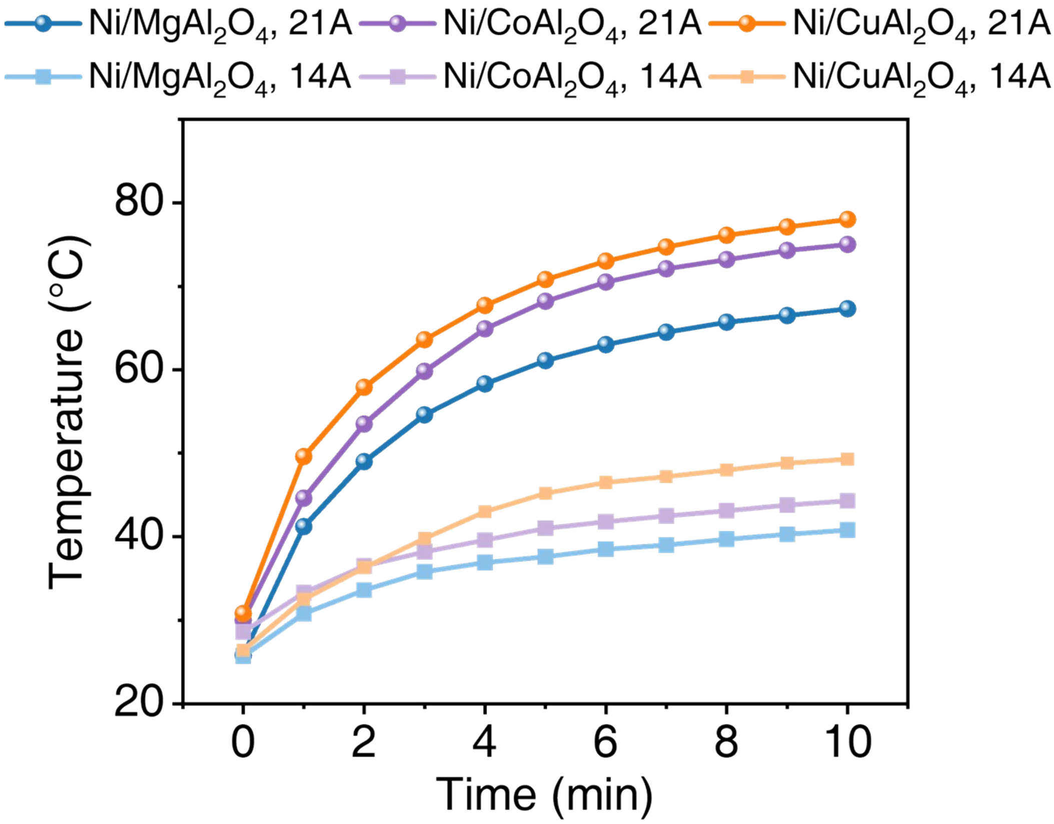

Figure S7. Effect of xenon lamp current on the temperature of $Ni/MgAl_2O_4$, $Ni/CoAl_2O_4$, and $Ni/CuAl_2O_4$ (Reaction conditions: 600 °C, GHSV = 12000 $mL \cdot g^{-1} \cdot h^{-1}$).

Table S1. Mass fraction of Ni in the catalyst.

Catalyst	Actual loading amount of Ni
	wt%
Ni/$MgAl_2O_4$	2.93
Ni/$CoAl_2O_4$	2.94
Ni/$CuAl_2O_4$	2.91

Table S2. The specific surface area, pore volume, and average pore diameter of $Ni/MgAl_2O_4$, $Ni/CoAl_2O_4$, and $Ni/CuAl_2O_4$.

Catalyst	**Specific surface area ($m^2 \cdot g^{-1}$)**	**Pore volume ($cm^3 \cdot g^{-1}$)**	**Average pore diameter (nm)**
$Ni/MgAl_2O_4$	181.29	0.16	13.37
$Ni/CoAl_2O_4$	52.8	0.22	17.58
$Ni/CuAl_2O_4$	44.81	0.12	7.45

Table S3. Relative amounts of oxygen vacancies in $Ni/MgAl_2O_4$, $Ni/CoAl_2O_4$, and $Ni/CuAl_2O_4$ calculated from XPS results.

Catalyst	**Oxygen vacancy content**
	O_V / (O_L + O_V + O_C)
$Ni/MgAl_2O_4$	32.06%
$Ni/CoAl_2O_4$	59.29%
$Ni/CuAl_2O_4$	58.26%

Table S4. Reaction rates of $Ni/CuAl_2O_4$, $Ni/CoAl_2O_4$, and $Ni/MgAl_2O_4$ catalysts in the TC-DRM and PTSC-DRM reactions (Reaction conditions: 600 °C, the light intensity is 2.91 $W\cdot cm^{-2}$, GHSV = 12000 $mL\cdot g^{-1}\cdot h^{-1}$).

Catalyst	**Reaction rates ($mL\cdot g^{-1}\cdot h^{-1}$)**			
	PTSC-CH_4	**TC-CH_4**	**PTSC-CO_2**	**TC-CO_2**
$Ni/CuAl_2O_4$	1299.72	758.58	1587	1122.25
$Ni/CoAl_2O_4$	5489.2	3878.58	5545.8	3962.58
$Ni/MgAl_2O_4$	4618.54	2438.58	5055.16	3027.78

Table S5. Selectivity of $Ni/CuAl_2O_4$, $Ni/CoAl_2O_4$, and $Ni/MgAl_2O_4$ catalysts in TC/PTSC-DRM reactions (Reaction conditions: 600 °C, the light intensity is 2.91 $W\cdot cm^{-2}$, GHSV = 12000 $mL\cdot g^{-1}\cdot h^{-1}$).

Catalyst	**H_2/CO**	
	PTSC	**TC**
$Ni/CuAl_2O_4$	0.77	0.62
$Ni/CoAl_2O_4$	0.99	0.97
$Ni/MgAl_2O_4$	0.96	0.87

Table S6. Carbon deposition of $Ni/MgAl_2O_4$ and $Ni/CoAl_2O_4$ after TC and PTSC reactions.

Catalyst	**Reaction time**	**Detection quality**	**Weight loss**	**Carbon deposit amount**	**Carbon deposition rate**
	(h)	**(mg)**	**(%)**	**(mg)**	**($mg \cdot h^{-1}$)**
$Ni/MgAl_2O_4$-PTSC	68.25	4.864	68.41	3.33	0.049
$Ni/MgAl_2O_4$-TC	19.5	4.532	63.39	2.87	0.15
$Ni/CoAl_2O_4$-PTSC	9.75	4.116	60.17	2.48	0.25
$Ni/CoAl_2O_4$-TC	6.5	4.837	67.2	3.25	0.5